Separation and Purification Technology 299 (2022) 121810

Contents lists available at ScienceDirect

Separation and Purification Technology

journal homepage: www.elsevier.com/locate/seppur

Cavitating substrates to boost water permeance of reverse osmosis membranes

Hao Yang [a], Zhe Zhang [b], Yong Wang [b,*]

[a] College of Chemistry & Chemical Engineering, Yantai University, Yantai 264005, Shandong, PR China
[b] State Key Laboratory of Materials-Oriented Chemical Engineering, College of Chemical Engineering, Nanjing Tech University, Nanjing 211816, Jiangsu, PR China

ARTICLE INFO

Keywords:
Block copolymers (BCPs)
Selective swelling
Reverse osmosis
Substrate
Interfacial polymerization

ABSTRACT

Reverse osmosis membranes have been shown to achieve reliable freshwater supply by means of water desalination. Nevertheless, breaking the long-standing trade-off is a major challenge for realizing high-efficient desalination. Herein, we show that selective swelling of substrates made by a block copolymer, polysulfone-*block*-poly(ethylene glycol) (PSF-*b*-PEG), is very promising in the fabrication of high-flux reverse osmosis membranes. Polyamide layers are first formed on relatively dense PSF-*b*-PEG substrates by interfacial polymerization. Then, the substrates are cavitated into highly porous substrates by selective swelling, which follows the mechanism of selective swelling-induced pore generation. The substrate porosity can be well tuned over a wide range via adjusting swelling duration. Selective swelling does not compromise the structural integrity and surface properties of polyamide layers atop the substrates. Importantly, the boosted porosity reduces the water transport resistance in substrates markedly, which in turn enables fast water permeation in reverse osmosis membranes. Thus, the optimal membrane shows exceptional water permeance of 50.4 L m^{-2} h^{-1} MPa^{-1} and a high NaCl rejection of 99.2%. Our work not only offers a novel strategy to enhance the water permeance of reverse osmosis membranes, but also demonstrates that the transport resistance of substrates also significantly influences water permeance of reverse osmosis membranes.

1. Introduction

Desalination of brackish groundwater and seawater by reverse osmosis (RO) has attracted considerable interest in providing freshwater. This technique is distinguished for its high efficacy, small footprint and flexible operation, compared with those of energy-intensive separation processes including distillations and evaporations [1–3]. Thin-film composite (TFC) is a generally adopted structure for most of RO membranes, which is composed of a polyamide layer and a porous substrate [4,5]. TFC membranes are prepared by interfacial polymerization, in which the rapid and irreversible reaction between diamines and acyl chlorides occurs at the interface of two immiscible phases [6–8]. Generally, the aqueous phase and organic phase are obtained by dissolving *m*-phenylenediamine (MPD) in water and trimesoyl chloride (TMC) in a liquid aliphatic hydrocarbon, respectively. Porous substrates are saturated with the aqueous phase, after which the organic phase contacts with the aqueous phase, initiating the reaction. Thus, the polyamide layers with high cross-linking density are formed on the top of the porous substrates. In light of the inherently fast reaction between MPD and TMC [9–11], such rebellious interfacial polymerization is very challenging to control, resulting in thick or even defective polyamide layers. This inevitably poses a trade-off between water permeance and salt rejection that would impair desalination performances [12,13]. Thus far, enhancing the water permeance while maintaining a high salt rejection, remains a challenge in the fabrication of high-performance desalination membranes.

The structural optimization of the polyamide layers is an explicit strategy for enhancing the water permeance of TFC membranes. For instance, thinning the thickness of polyamide layers has shown to alleviate the transport resistance of water in polyamide layers, which facilitates the water permeation [14–17]. Alternatively, doping the nanofillers into polyamide layers creates nanogaps serving as additional transport channels, which is effective for facilitating the water permeation [18–21]. Under such circumstances, however, the decline of salt rejections inevitably occurs, because the integrity of polyamide layers is susceptible to the reduction of the thickness and the incorporation of nanofillers. It is noteworthy that water transport across TFC membranes depends on not only the dense polyamide layers, but also the substrates

* Corresponding author.
E-mail address: yongwang@njtech.edu.cn (Y. Wang).

https://doi.org/10.1016/j.seppur.2022.121810
Received 19 June 2022; Received in revised form 22 July 2022; Accepted 23 July 2022
Available online 26 July 2022

[22]. The surface porosity of the substrate influences the transport distance of water in transverse direction inside the polyamide layers [14]. The low surface porosity makes water transport difficult, as it requires much longer transverse distance that enables the transport from the polyamide layers to the pore openings of the substrates [23]. Improving the surface porosity, the transverse distance for water transport between the polyamide layers and the pore openings of the substrate can be shortened sharply. In other words, the high surface porosity offers a large number of shortcuts in normal direction that confers the fast permeation of water from polyamide layers to substrates [23]. This strategy opens up an avenue for boosting the water permeance without compromising the integrity of polyamide layers.

It should be noted that the substrate is of vital significance to the formation of polyamide layers [22–24]. Their porosities influence the uptake and the release of diamines for the interfacial polymerization [25–27]. Therefore, it would be a nimble way that the porosity of the substrate can be improved after the formation of polyamide layers. Swelling of block copolymers using selective solvents is a highly easy and efficient approach to create nanoporous materials, which is known as selective swelling-induced pore generation [28–32]. In a typical process, dense and continuous films made by block copolymer are soaked into selective solvent which exhibit high affinity to the minority domains. The minority domains uptake the selective solvent quickly, and the osmotic pressure inside the domains begins to rise. The accumulated osmotic pressure enables the minority domains to expand, so that they can overflow from the interior to the film surface [28]. Meanwhile, since the majority domains are slightly swollen and gain adequate mobility by the selective solvent, the expanded minority domains further squeeze the majority ones, thus enlarging the volume of the minority domains. After drying at room temperature, the minority domains collapse and attach onto the majority ones whose mobility has been frozen. As a result, the positions pre-occupied by the minority domains are converted into interconnected nanoporosity [28]. Given the unique way in pore generation, we envision that it can essentially improve the porosity of the substrate made by block copolymers in a nondestructive way.

In this work, we develop a novel strategy using block copolymer as the substrate for the preparation of high-performance RO membranes (Scheme 1). A block copolymer, polysulfone-*block*-poly(ethylene glycol) (PSF-*b*-PEG), is spin-coated onto a macroporous support to prepare the substrate. Then, the polyamide layers are formed atop the substrate by interfacial polymerization of MPD and TMC. Thus-obtained membranes are subjected to selective swelling for the cavitation of the substrates. It is found that the relatively dense PSF-*b*-PEG substrates can be converted into highly porous substrates with the principle of selective swelling-induced pore generation. Importantly, such process does not compromise the physical and chemical structures of the polyamide layers. By changing the duration of selective swelling, the porosity (overall porosity) as well as the separation performance of PSF-*b*-PEG substrates are well adjusted. Thus, the boosted porosity enables large water permeances, for instance, the optimal membrane shows water permeance of up to 50.4 L m^{-2} h^{-1} MPa^{-1}, along with NaCl rejection of 99.2%. This work demonstrates the applicability of selective swelling of block copolymers in fabricating RO membranes. Furthermore, it also reveals that the water transport resistance in substrates plays a vital role in deciding the water permeation in RO membranes.

2. Experimental section

2.1. Materials

PSF-*b*-PEG (M_n = 791,000 g mol^{-1}, polydispersity index = ~2.0) was provided by Nanjing Bangding. The weight ratio of PEG was 21%. *m*-Phenylenediamine (MPD, 99.5%), trimesoyl chloride (TMC, 98%) and *n*-hexane (HPLC grade) were purchased from Sigma-Aldrich. 1,2-Dichloroethane (99.5%), acetone (99.5%), ethanol (99.7%) and sodium chloride (NaCl, 99.8%) were obtained from Sinopharm Chemical Reagent Co., Ltd. Phosphate buffered saline (PBS) tablets and bovine serum albumin (BSA) were purchased from MP Biomedicals. Silicon wafers and hydrophilic polyvinylidene fluoride membranes (PVDF, mean pore size = 220 nm, Durapore, Millipore) were used as the smooth substrate and the macroporous support, respectively. Deionized water with the conductivity being less than 5 μS cm^{-1} was homemade. All chemical reagents were used without further treatment.

2.2. Preparation of PSF-b-PEG substrates

The PSF-*b*-PEG solution with a concentration of 1 wt% was obtained via dissolving PSF-*b*-PEG in 1,2-dichloroethane. Then, the solution was filtrated using polytetrafluoroethylene filters (mean pore size = 220 nm, Jinteng) to remove insoluble impurities. The PSF-*b*-PEG substrates were fabricated via spin-coating of the polymer solutions onto PVDF

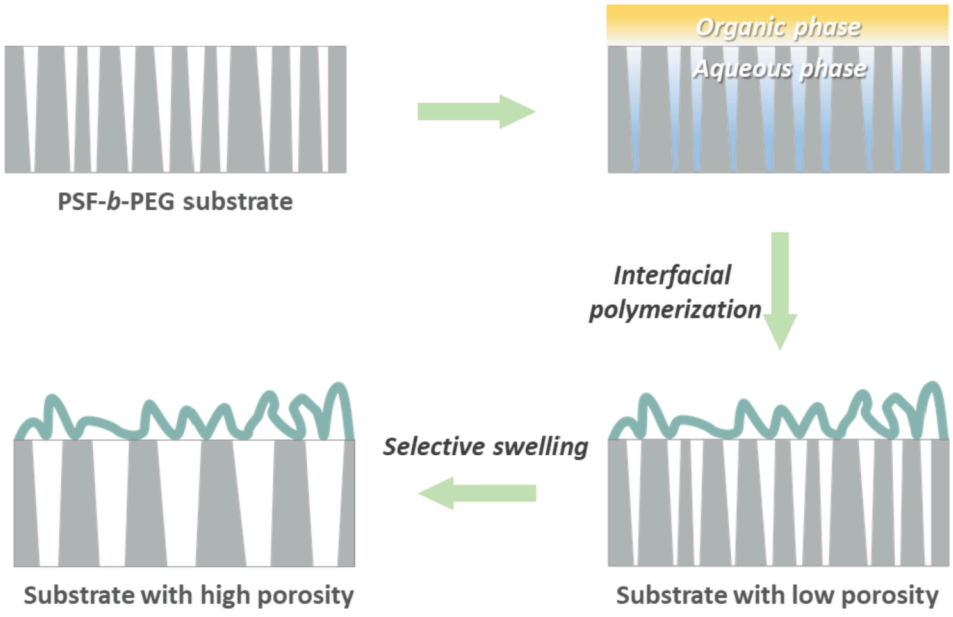

Scheme 1. Schematic exhibiting the preparation of the high-flux TFC membrane via selective swelling of the substrate made by a block copolymer.

macroporous supports. Before spin-coating, the macropore of PVDF supports were pre-filled with water to prevent the intrusion of polymer solutions. Typically, 400 μL of PSF-*b*-PEG solutions were dropped onto the upper surface of water-filled PVDF supports, followed by the spin-coating at 2000 rpm for 30 s. The thin films of PSF-*b*-PEG atop the PVDF supports can be obtained, after the evaporation of 1,2-dichloroethane.

2.3. TFC membranes prepared on PSF-b-PEG substrates

The TFC membranes were obtained via interfacial polymerization with the PSF-*b*-PEG substrates. First, the PSF-*b*-PEG substrates were immersed into 4 wt% of MPD for 1 min. The excess MPD solution on the substrates was carefully removed by wiping papers. Then, the 0.2 wt% of TMC were slowly poured on the upper surface of the PSF-*b*-PEG substrates. After a reaction duration of 2 min, the residual solutions were removed, and the PSF-*b*-PEG substrates were heated at 80 °C for 10 min. Whereafter, the TFC membranes were soaked into a solvent mixture containing acetone and ethanol (v/v, 1:19) at 40 °C for designated durations, to implement the selective swelling process. After that, the TFC membranes were dried at room temperature for further use. Note that, for characterization, thin films of PSF-*b*-PEG were also prepared using silicon wafers as the substrate, and the procedures regarding the preparation and selective swelling were the same as above.

2.4. Characterizations

The microstructures of PSF-*b*-PEG substrates and TFC membranes were analyzed by scanning electron microscopy (SEM, Hitachi S-4800) including the surface and cross-sectional morphologies of membranes. Before testing, the membranes were sputtered coated with platinum to improve the conductivity. The surface roughness of TFC membranes was characterized by atomic force microscopy (AFM, XE-100, Park Systems). Water contact angles (WCAs) of TFC membranes were recorded on a Drop Meter A100P goniometer (MAIST). Attenuated total reflectance Fourier transform infrared spectroscopy (ATR-FTIR, Nicolet 8700, Thermo Fisher Scientific) was used to characterize the chemical compositions of PSF-*b*-PEG substrates and TFC membranes. The porosity of PSF-*b*-PEG thin films on silicon wafers was measured by spectroscopic ellipsometry (Complete EASEM-2000U, J. A. Woollam) at an incidence angle of 70°. The porosity (Φ_{pore}) can be calculated as follows [33]:

$$n^2_{\text{after swelling}} = n^2_{\text{before swelling}}\left(1-\Phi_{\text{pore}}\right) + n^2_{\text{air}}\Phi_{\text{pore}} \quad (1)$$

where $n_{\text{before swelling}}$ and $n_{\text{after swelling}}$ are the refractive index of PSF-*b*-PEG thin film before and after selective swelling, respectively. n_{air} is the refractive index of air of 1.

2.5. Separation performance evaluation

The permeance as well as the rejection of BSA and NaCl were measured on a cross-flow filtration device (SF-SB, Hangzhou Saifei Membrane Separation Co., Ltd.). The hydraulic pressures for the test of PSF-*b*-PEG substrates and TFC membranes were both fixed at 0.7 MPa. The liquid temperature was 25 °C throughout the test. The membranes were stabilized at 0.7 MPa for 30 min to acquire steady permeance. The concentration of BSA aqueous solution was 500 ppm (PBS was used as the buffer), and the concentration was determined by an UV–vis spectrophotometer (Nanodrop 2000c, Thermo Fisher Scientific). The concentration of NaCl aqueous solution was 2000 ppm, and the concentration was determined by a conductivity meter (S230-K, Mettler-Toledo). The separation performances were calculated as following:

$$J = \Delta V/(A\Delta t) \quad (2)$$

$$P_w = \Delta V/(A\Delta t\Delta p) \quad (3)$$

$$R = (1 - C_p/C_f) \times 100\% \quad (4)$$

where J (L m^{-2} h^{-1}) is the water flux, P_w (L m^{-2} h^{-1} bar^{-1}) is the water permeance, R (%) are the rejection of BSA and NaCl, V (L) is the permeated solution volume, A (m^2) is the active area, Δt (h) is the permeation duration, and Δp (bar) is the hydraulic pressure, respectively. C_p and C_f are the concentrations of BSA or NaCl in the permeated solution and the feed, respectively.

3. Results and discussion

3.1. Preparation and characterization of membranes

In this work, selective swelling-induced pore generation process is applied to boost the porosity of PSF-*b*-PEG substrates after the formation of polyamide layers. It is expected that this unique strategy can markedly enhance the water permeance, while maintaining a high rejection of NaCl. To highlight the necessity of this strategy, we tried to implement the interfacial polymerization directly on the PSF-*b*-PEG substrates after selective swelling. In PSF-*b*-PEG, PEG is the minor domain, which would wrap the major domain of PSF after selective swelling [30]. Due to the strong hydration property of PEG, the surface hydrophilicity of substrates would be greatly improved after selective swelling [30,34]. Thus, accompanied with the boosted porosity, the strong hydrophilicity makes the formation of polyamide layers very difficult [35]. The strong hydrophilicity restricts the diffusion of MPD toward the TMC solution, resulting in the intrusion of polyamide to the nanopores of the substrate [36–38]. This consequentially leads to the formation of defects, and the resultant TFC membranes would fail to give satisfactory rejection to NaCl. To circumvent such obstacle, the process of selective swelling was implemented after the formation of polyamide layers.

To validate the occurrence of selective swelling-induced pore generation, we first used SEM to examine the surface morphology of PSF-*b*-PEG thin films prepared on silicon wafers under different selective swelling durations. As shown in Fig. 1a-f, after selective swelling, all surfaces of PSF-*b*-PEG thin films are highly porous regardless of selective swelling durations. We further used ellipsometry to calculate the porosity of PSF-*b*-PEG thin films in terms of the refractive index. As shown in Fig. 1g, with the progress of selective swelling, the porosity and the pore size of PSF-*b*-PEG layers both drastically increased. Prolonging the duration of selective swelling, the PEG domains can be strongly swollen and markedly expanded. The PSF domains would be squeezed by the extended PEG domains to a large extent, and more PEG domains can overflow from the interior to the surface, thus leaving higher porosity and larger pore size after drying at room temperature. This indicates that the porosity and pore size of PSF-*b*-PEG thin films can be tuned by adjusting the duration of selective swelling. Above results provide direct evidence to the occurrence of the process of selective swelling-induced pore generation.

We then checked the morphologies of TFC membranes with various selective swelling durations by SEM (Fig. 2). All membranes have similar morphology including surface and cross-sectional structures. They possess the leave-like and highly crumpled polyamide layers, which exhibit the ridge-and-valley structure [8]. The formation of such structure originates from the vigorous heat dissipation at the interface by the fast and irreversible interfacial polymerization [14]. Above results illustrate that the polyamide layers were successful formed on the PSF-*b*-PEG substrate. After the implementation of selective swelling at 40 °C for 0.5 and 8 h, the ridge-and-valley structure still maintained in both TFC membranes. In addition, the pristine membrane and the membranes after selective swelling all have a similar intrinsic thickness of ~29 nm, which are obtained from the cross section of those membranes. The polyamide layers are tightly attached on the PSF-*b*-PEG substrates, and do not peel off from the substrates after selective swelling. AFM images display that the surface morphology of TFC membranes before and after

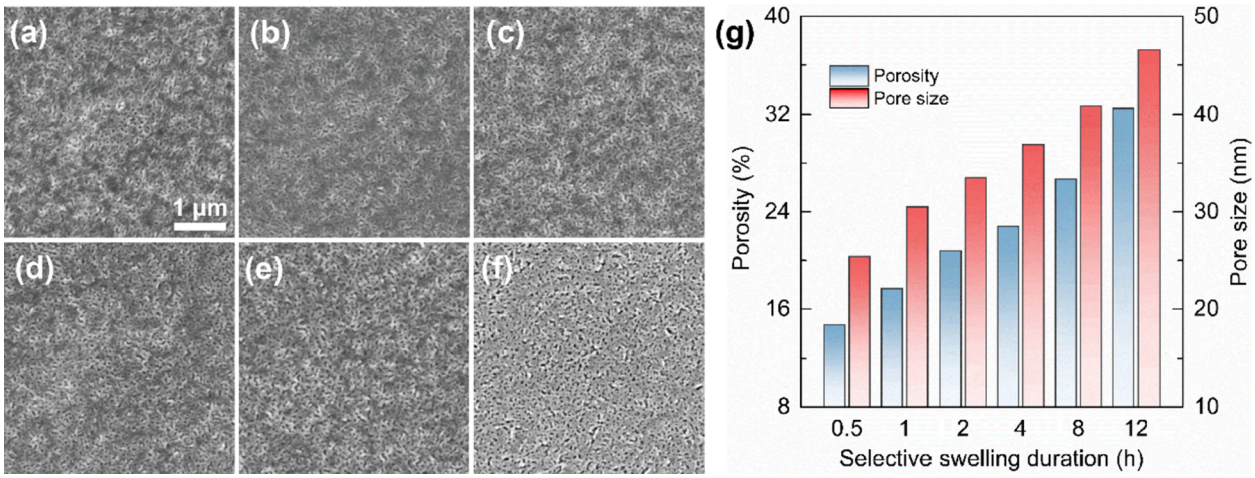

Fig. 1. Validation of selective swelling-induced pore generation. SEM images of the surface morphologies of PSF-*b*-PEG thin films prepared on silicon wafers under different selective swelling durations for 0.5 h (a), 1 h (b), 2 h (c), 4 h (d), 8 h (e). and 12 h (f). The scale bar in Fig. 1a applies to all images. (g) Variations of the porosity and pore size of PSF-*b*-PEG thin films under different selective swelling durations.

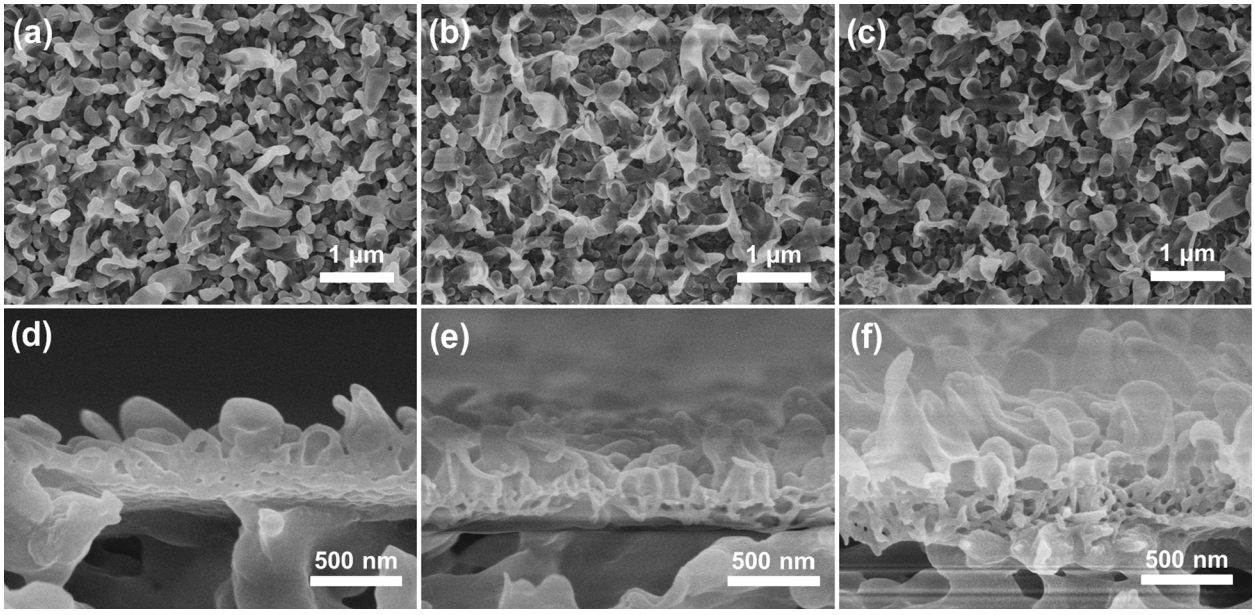

Fig. 2. SEM images of the morphologies of TFC membranes. The surface (a-c) and the cross-sectional (d-f) morphologies of the TFC membranes obtained without selective swelling (a, d) and with a selective swelling duration for 0.5 h (b, e), and 8 h (c, f).

selective swelling are in almost same (Fig. S1). Notably, the PVDF support possesses solvent and heat resistances, which would not be compromised under the conditions of selective swelling [34]. Therefore, selective swelling does not influence the microstructure of the polyamide layers and the structural integrity of the TFC membranes.

3.2. Surface properties of membranes

To disclose the influence of selective swelling on surface properties of TFC membranes, ATR-FTIR characterizations and WCAs tests were carried out. ATR-FTIR spectra demonstrate the surface chemical composition of the substrate and the TFC membranes (Fig. 3a). The characteristic peaks of C=O (1662 cm^{-1} and 1609 cm^{-1}) and N-H (1543 cm^{-1}) assigned to the polyamide appeared in all spectra of TFC membranes, compared with those of the substrate. Note that characteristic peaks around 1155 cm^{-1}, 1235 cm^{-1} and 1102 cm^{-1}, were ascribed to the sulfone and ether groups of the PSF-*b*-PEG substrates, and no obvious change appeared before and after selective swelling. This is clearly indicative of the formation of polyamide layers by the interfacial polymerization. Furthermore, after the process of selective swelling, those characteristic peaks remained almost unchanged. As shown in Fig. 3b, WCAs of the TFC membrane prepared with different swelling durations varied slightly in the range of ~60-65°, suggesting that they all have nearly identical surface hydrophilicity. Overall, it can be concluded that the surface properties of the polyamide layers do not change noticeably after the process of selective swelling.

3.3. Separation performances of membranes

To probe the relationship between membrane structure and separation performance, we evaluated the separation performances of the PSF-*b*-PEG substrates and the TFC membranes. The separation performances of PSF-*b*-PEG substrates with selective swelling under various durations are shown in Fig. 4a. The substrate without selective swelling possessed a low water permeance of 64 L m^{-2} h^{-1} MPa^{-1}, and a high BSA rejection of 98.6%. When the swelling time was 2 h, the water permeance

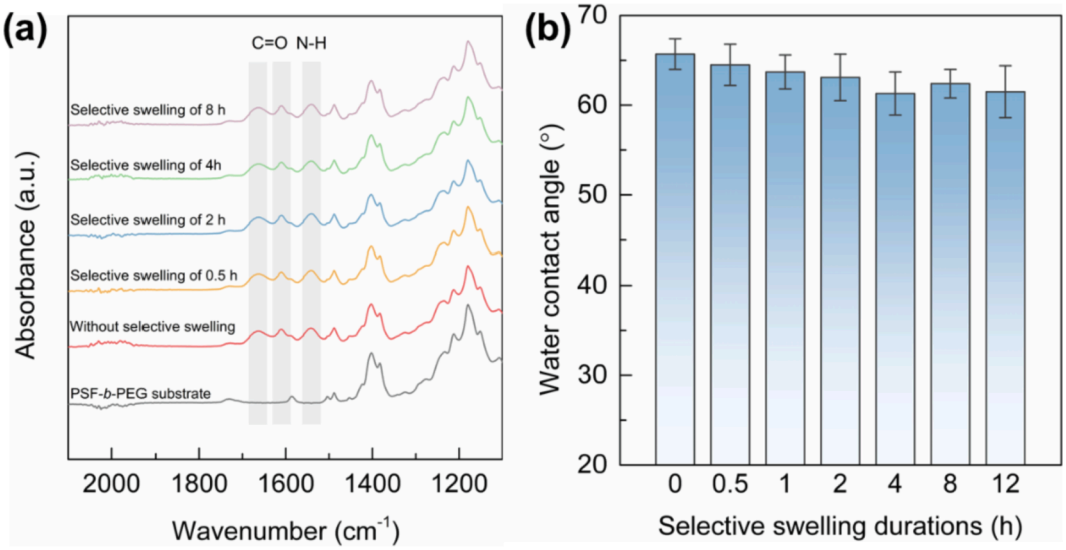

Fig. 3. Surface properties of PSF-*b*-PEG substrates and TFC membranes. (a) FTIR spectra (b) WCAs.

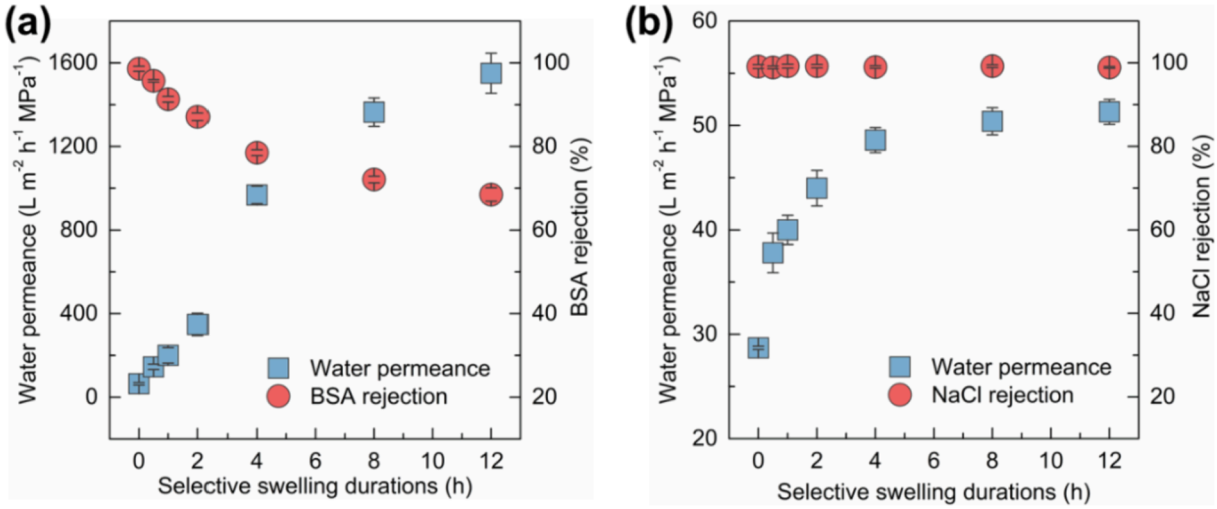

Fig. 4. Separation performances of different membranes under various selective swelling durations. (a) PSF-*b*-PEG substrates. (b) TFC membranes.

progressively increased to 348 L m^{-2} h^{-1} MPa^{-1} and BSA rejection decreased to 87.1%. When the swelling time reached 4 h, the water permeance drastically increased to 968 L m^{-2} h^{-1} MPa^{-1} and BSA rejection declined to 78.5%. Further, with the duration of 8 h, the water permeance was 1364 L m^{-2} h^{-1} MPa^{-1} and BSA rejection was 72.1%. Finally, with the duration of 12 h, the water permeance increased to 1550 L m^{-2} h^{-1} MPa^{-1}, and BSA rejection declined to 68.5%. The substrate without selective swelling showed a low water permeance because of its low porosity. With the progress of selective swelling, the water permeance increased along with the decline of the BSA rejections. This can be attributed to the porosity boosted by selective swelling. Therefore, the variation of the separation performances can be well related to the changes of the porosity of the substrates. This phenomenon also suggests that the separation performances can be tuned by the duration of selective swelling.

We then evaluated the desalination performance of TFC membranes prepared from the different PSF-*b*-PEG substrates. The TFC membrane without selective swelling exhibited low water permeance of 28.7 L m^{-2} h^{-1} MPa^{-1}, and a high NaCl rejection of 99.1% (Fig. 4b). This desalination performance is owing to the low water permeance of the substrate. With the progress of selective swelling, the water permeance progressively increased, and NaCl rejection almost maintained at a high level of around 99%. This is able to interpret by the progressively enhanced porosity of the substrate, as demonstrated before. The optimal desalination performance was obtained at the duration of 8 h. The TFC membrane presented a remarkably high water permeance of 50.4 L m^{-2} h^{-1} MPa^{-1} and NaCl rejection of 99.2%. Note that, the TFC membrane prepared from the duration of 12 h exhibited a somewhat larger water permeance of 51.3 L m^{-2} h^{-1} MPa^{-1}. Yet, it exhibited a slightly declined NaCl rejection of 98.9%. Thus, the tendency of the desalination performances is in line with that of the PSF-*b*-PEG substrates. Compared with most of other RO membranes, our membranes received exceptional desalination performance under a low operation pressure of 0.7 MPa. This would make our membranes very promising in the application of RO processes operated under low pressures that consume less energy and have large water production.

3.4. Analysis of the transport resistance

To understand the role of the porosity of the substrate on the enhancement of water permeance, we analyzed the transport resistance of water in TFC membranes. Considering that the polyamide layers have

a similar thickness, the substrates would also influence the transport resistance of water. According to Darcy's low [39,40], the transport resistance (R, m^{-1}) of water can be obtained as follows:

$$R = \Delta p/(\mu J) \quad (5)$$

where Δp (Pa) is the hydraulic pressure, μ (0.91×10^{-3} Pa s) is water viscosity, and J ($m^3\ m^{-2}\ s^{-1}$) is water flux, respectively. Therefore, we can use a resistance-in-series model to describe the transport resistance of water. The transport resistance of water in TFC membranes is composed of the resistance in polyamide layers (R_1) as well as the resistance in substrates (R_2) (Fig. 5a) [41]. As shown in Fig. 5b, with the progress of selective swelling, the transport resistance of water in TFC membranes began to decline. Given the nearly constant resistance assigned to the polyamide layers, the resistance attributed to the substrates displayed a sharp decrease. Specifically, the resistance in the substrate without selective swelling was 45.1%. With a duration of selective swelling for 0.5 h, the resistance decreased to 26.1%. Moreover, the resistance was merely 3.7%, when the optimal duration of selective swelling appeared. Above results are mainly because of the improved the porosity shortening the transverse distance for water transport between the polyamide layers and the pore openings [14,23]. This would confer adequate shortcuts in normal direction that allows water to transport much easily from the polyamide layers into the substrates.

In addition, we also used the permeance ratio to quantify the transport resistance of water (Fig. 5c). Permeance ratio was defined as the ratio of the permeance of substrates by the permeance of TFC membranes, under the same duration of selective swelling. The permeance ratios were sharply increased, as the duration of selective swelling exceeded 2 h. This tendency is well in line with that of the transport resistance analysis. Therefore, the resistance in substrates is crucial for the transport of water through TFC membranes, and it should not be overlooked. The above results also underline that the highly-permeable substrates originating from the high porosity are necessary for the preparation of high-flux TFC RO membranes.

4. Conclusion

In conclusion, we develop a unique strategy by using a block copolymer, PSF-*b*-PEG, as the substrate to fabricate high-flux RO membranes. After the formation of polyamide layers on the pristine PSF-*b*-PEG substrates, thus-obtained TFC membranes are subjected to selective swelling. According to the principle of selective swelling-induced pore generation, the pristine PSF-*b*-PEG substrates can be converted into highly porous substrates. Importantly, this process does not compromise the integrity, morphologies and the surface properties of the polyamide layers. The porosity and the separation performance of PSF-*b*-PEG substrates can be well tuned via adjusting the duration of selective swelling. Due to the reduced water transport resistance in substrates, the water permeance of TFC membranes is significantly boosted, while still holding a high rejection to NaCl. Under the optimal duration of selective swelling, the TFC membrane presents a remarkably large water permeance of 50.4 L m^{-2} h^{-1} MPa^{-1} and a high NaCl rejection of 99.2%. Notably, the exceptional desalination performances received under a low pressure of 0.7 MPa makes our membranes very promising in the application of low-pressure RO. Our work demonstrates the feasibility and superiority of selective swelling of block copolymers in the fabrication of RO membranes. Also, this work underlines that the water transport resistance in substrates should not be overlooked.

CRediT authorship contribution statement

Hao Yang: Methodology, Investigation, Writing – original draft, Funding acquisition. **Zhe Zhang:** Writing – review & editing. **Yong Wang:** Supervision, Writing – review & editing, Funding acquisition.

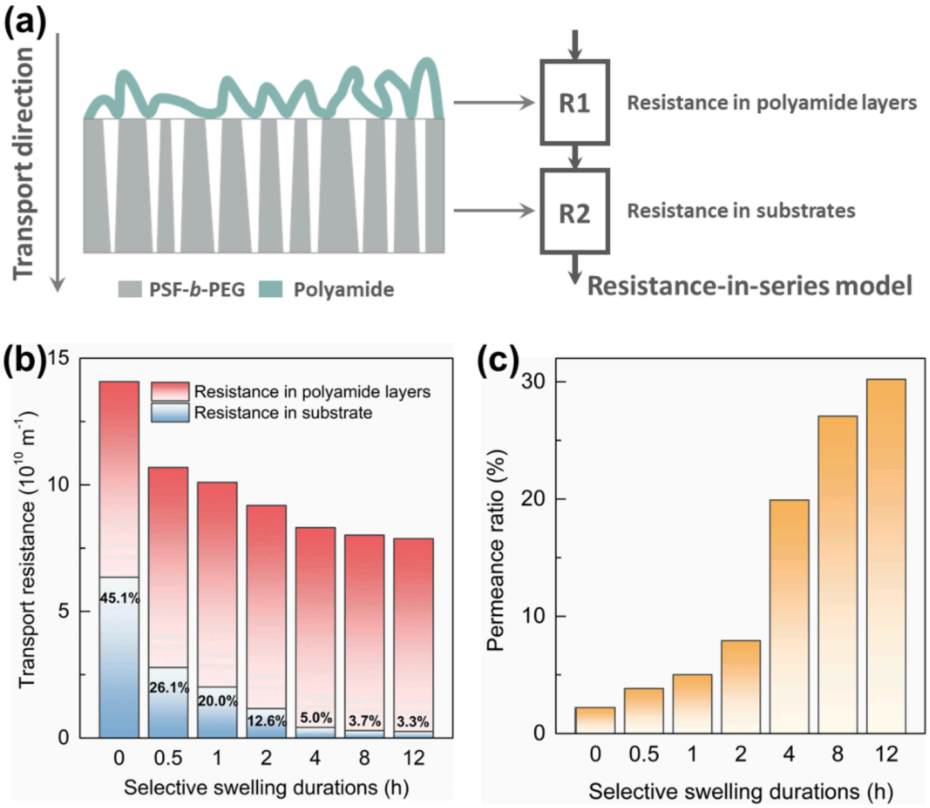

Fig. 5. Analysis of the transport resistance. (a) The schematic depiction of the transport resistances. (b) The transport resistance of TFC membranes under different durations of selective swelling. (c) The permeance ratio of TFC membranes under different durations of selective swelling.

Declaration of Competing Interest

The authors declare that they have no known competing financial interests or personal relationships that could have appeared to influence the work reported in this paper.

Acknowledgements

Financial support from the National Basic Research Program of China (2015CB655301) is acknowledged. H. Y. thanks the National Natural Science Foundation of China (52103270 and 22108233), the Shandong Natural Science Foundation (ZR2020QB176) and the Shandong Key Research and Development Program (2019JZZY010410).

Appendix A. Supplementary data

Supplementary data to this article can be found online at https://doi.org/10.1016/j.seppur.2022.121810.

References

[1] M.A. Shannon, P.W. Bohn, M. Elimelech, J.G. Georgiadis, B.J. Mariñas, A. M. Mayes, Science and technology for water purification in the coming decades, Nature 452 (7185) (2008) 301–310.
[2] J.R. Werber, C.O. Osuji, M. Elimelech, Materials for next-generation desalination and water purification membranes, Nat. Rev. Mater. 1 (2016) 16018.
[3] M. Qasim, M. Badrelzaman, N.N. Darwish, N.A. Darwish, N. Hilal, Reverse osmosis desalination: a state-of-the-art review, Desalination 459 (2019) 59–104.
[4] Y.J. Lim, K. Goh, M. Kurihara, R. Wang, Seawater desalination by reverse osmosis: current development and future challenges in membrane fabrication-a review, J. Membr. Sci. 629 (2021) 119292.
[5] Y. Yao, P. Zhang, C. Jiang, R.M. DuChanois, X. Zhang, M. Elimelech, High performance polyester reverse osmosis desalination membrane with chlorine resistance, Nat. Sustain. 4 (2) (2021) 138–146.
[6] M.J.T. Raaijmakers, N.E. Benes, Current trends in interfacial polymerization chemistry, Prog. Polym. Sci. 63 (2016) 86–142.
[7] F. Zhang, J.-B. Fan, S. Wang, Interfacial polymerization: from chemistry to functional materials, Angew. Chem. Int. Ed. 59 (49) (2020) 21840–21856.
[8] X. Lu, M. Elimelech, Fabrication of desalination membranes by interfacial polymerization: history, current efforts, and future directions, Chem. Soc. Rev. 50 (2021) 6290–6307.
[9] E.L. Wittbecker, P.W. Morgan, Interfacial polycondensation. I, J. Polym. Sci. 40 (1959) 289–297.
[10] P.W. Morgan, S.L. Kwolek, Interfacial polycondensation. II. Fundamentals of polymer formation at liquid interfaces, J. Polym. Sci. 40 (1959) 299–327.
[11] Z. Tan, S. Chen, X. Peng, L. Zhang, C. Gao, Polyamide membranes with nanoscale Turing structures for water purification, Science 360 (6388) (2018) 518–521.
[12] B. Park Ho, J. Kamcev, M. Robeson Lloyd, M. Elimelech, D. Freeman Benny, Maximizing the right stuff: the trade-off between membrane permeability and selectivity, Science 356 (2017) eaab0530.
[13] Z. Yang, H. Guo, C.Y. Tang, The upper bound of thin-film composite (TFC) polyamide membranes for desalination, J. Membr. Sci. 590 (2019) 117297.
[14] Z. Jiang, S. Karan, A.G. Livingston, Water transport through ultrathin polyamide nanofilms used for reverse osmosis, Adv. Mater. 30 (2018) 1705973.
[15] B. Gan, S. Qi, X. Song, Z. Yang, C.Y. Tang, X. Cao, Y. Zhou, C. Gao, Ultrathin polyamide nanofilm with an asymmetrical structure: a novel strategy to boost the permeance of reverse osmosis membranes, J. Membr. Sci. 612 (2020) 118402.
[16] Q. Shen, Y. Lin, T. Ueda, P. Zhang, Y. Jia, T. Istirokhatun, Q. Song, K. Guan, T. Yoshioka, H. Matsuyama, The underlying mechanism insights into support polydopamine decoration toward ultrathin polyamide membranes for high-performance reverse osmosis, J. Membr. Sci. 646 (2022) 120269.
[17] Y. Wen, R. Dai, X. Li, X. Zhang, X. Cao, Z. Wu, S. Lin, C.Y. Tang, Z. Wang, Metal-organic framework enables ultraselective polyamide membrane for desalination and water reuse, Sci. Adv. 8 (2022) eabm4149.
[18] B.-H. Jeong, E.M.V. Hoek, Y. Yan, A. Subramani, X. Huang, G. Hurwitz, A. K. Ghosh, A. Jawor, Interfacial polymerization of thin film nanocomposites: a new concept for reverse osmosis membranes, J. Membr. Sci. 294 (2007) 1–7.
[19] L.i. Yu, W. Zhou, Y. Li, Q. Zhou, H. Xu, B. Gao, Z. Wang, Antibacterial thin-film nanocomposite membranes incorporated with graphene oxide quantum dot-mediated silver nanoparticles for reverse osmosis application, ACS Sustainable Chem. Eng. 7 (9) (2019) 8724–8734.
[20] G. Yang, Z. Zhang, C. Yin, X. Shi, Y. Wang, Polyamide membranes enabled by covalent organic framework nanofibers for efficient reverse osmosis, J. Polym. Sci. 1 (2021), https://doi.org/10.1002/pol.20210664.
[21] X. Dong, X. Wang, H. Xu, Y. Huang, C. Gao, X. Gao, Mesoporous hollow nanospheres with amino groups for reverse osmosis membranes with enhanced permeability, J. Membr. Sci. 657 (2022) 120637.
[22] J. Li, M. Wei, Y. Wang, Substrate matters: The influences of substrate layers on the performances of thin-film composite reverse osmosis membranes, Chin. J. Chem. Eng. 25 (2017) 1676–1684.
[23] Z. Yang, P.-F. Sun, X. Li, B. Gan, L. Wang, X. Song, H.-D. Park, C.Y. Tang, A critical review on thin-film nanocomposite membranes with interlayered structure: mechanisms, recent developments, and environmental applications, Environ. Sci. Technol. 54 (2020) 15563–15583.
[24] L.E. Peng, Z. Yao, Z. Yang, H. Guo, C.Y. Tang, Dissecting the role of substrate on the morphology and separation properties of thin film composite polyamide membranes: seeing is believing, Environ. Sci. Technol. 54 (11) (2020) 6978–6986.
[25] L. Huang, J.R. McCutcheon, Impact of support layer pore size on performance of thin film composite membranes for forward osmosis, J. Membr. Sci. 483 (2015) 25–33.
[26] Q. Zhang, Z. Zhang, L. Dai, H. Wang, S. Li, S. Zhang, Novel insights into the interplay between support and active layer in the thin film composite polyamide membranes, J. Membr. Sci. 537 (2017) 372–383.
[27] Y. Zhao, G.S. Lai, Y. Wang, C. Li, R. Wang, Impact of pilot-scale PSF substrate surface and pore structural properties on tailoring seawater reverse osmosis membrane performance, J. Membr. Sci. 633 (2021) 119395.
[28] Y. Wang, F. Li, An emerging pore-making strategy: confined swelling-induced pore generation in block copolymer materials, Adv. Mater. 23 (2011) 2134–2148.
[29] Y. Wang, Nondestructive creation of ordered nanopores by selective swelling of block copolymers: toward homoporous membranes, Acc. Chem. Res. 49 (7) (2016) 1401–1408.
[30] Z. Wang, R. Liu, H. Yang, Y. Wang, Nanoporous polysulfones with in situ PEGylated surfaces by a simple swelling strategy using paired solvents, Chem. Commun. 53 (65) (2017) 9105–9108.
[31] J. Zhou, Y. Wang, Selective swelling of block copolymers: an upscalable greener process to ultrafiltration membranes? Macromolecules 53 (2020) 5–17.
[32] L. Guo, Y. Wang, M. Steinhart, Porous block copolymer separation membranes for 21st century sanitation and hygiene, Chem. Soc. Rev. 50 (11) (2021) 6333–6348.
[33] T.C. Choy, Effective medium theory: principles and application, Oxford University Press, New York, USA, 1999.
[34] H. Yang, J. Zhou, Z. Wang, X. Shi, Y. Wang, Selective swelling of polysulfone/poly (ethylene glycol) block copolymer towards fouling-resistant ultrafiltration membranes, Chin. J. Chem. Eng. 28 (1) (2020) 98–103.
[35] M. Fathizadeh, A. Aroujalian, A. Raisi, Effect of lag time in interfacial polymerization on polyamide composite membrane with different hydrophilic sub layers, Desalination 284 (2012) 32–41.
[36] Z. Yang, Z.-W. Zhou, H. Guo, Z. Yao, X.-H. Ma, X. Song, S.-P. Feng, C.Y. Tang, Tannic acid/Fe^{3+} nanoscaffold for interfacial polymerization: toward enhanced nanofiltration performance, Environ. Sci. Technol. 52 (2018) 9341–9349.
[37] Z. Zhou, Y. Hu, C. Boo, Z. Liu, J. Li, L. Deng, X. An, High-performance thin-film composite membrane with an ultrathin spray-coated carbon nanotube interlayer, Environ. Sci. Technol. Lett. 5 (5) (2018) 243–248.
[38] Y.J. Lim, K. Goh, G.S. Lai, Y. Zhao, J. Torres, R. Wang, Unraveling the role of support membrane chemistry and pore properties on the formation of thin-film composite polyamide membranes, J. Membr. Sci. 640 (2021) 119805.
[39] G.B. van den Berg, C.A. Smolders, Flux decline in ultrafiltration processes, Desalination 77 (1990) 101–133.
[40] X. Zhang, W. Zhou, F. Xu, M. Wei, Y. Wang, Resistance of water transport in carbon nanotube membranes, Nanoscale 10 (27) (2018) 13242–13249.
[41] K. Guan, Y. Sasaki, Y. Jia, R.R. Gonzales, P. Zhang, Y. Lin, Z. Li, H. Matsuyama, Interfacial polymerization of thin film selective membrane layers: effect of polyketone substrates, J. Membr. Sci. 640 (2021) 119801.